Uncommon Adsorption Isotherm of Methanol on a Hydrophobic Y-zeolite

ARTICLE *in* THE JOURNAL OF PHYSICAL CHEMISTRY B · OCTOBER 2001

Impact Factor: 3.3 · DOI: 10.1021/jp0103530

3 AUTHORS, INCLUDING:

Istvan Halasz
PQ Corporation
122 PUBLICATIONS **880** CITATIONS

Uncommon Adsorption Isotherm of Methanol on a Hydrophobic Y-zeolite

Istvan Halasz,* Song Kim, and Bonnie Marcus

Zeolyst International, R&D Center, 280 Cedar Grove Road, Conshohocken, Pennsylvania 19428

Received: January 26, 2001; In Final Form: July 25, 2001

The physisorption of methanol vapor on a dealuminated, commercial Y type zeolite (CBV-901) at temperatures from 0 to 80 °C, produces a rare Type V adsorption isotherm. In contrast to some microporous carbons and $AlPO_4$-5 derivatives that give Type V isotherms only with water, CBV-901 barely adsorbs water at $p/p_o <$ 0.7 relative pressures. Micropore filling with methanol takes place near $p/p_o \approx 0.2$, which is unusually low for Type V isotherms. To our knowledge, such isotherms have not been reported over zeolites before. Pore size measurements and grand canonical Monte Carlo molecular simulation experiments indicate that the selective micropore condensation of methanol is intimately associated with the micropore structure and the force field of the dealuminated Y-zeolite. Mesopores or lattice defects including silanol groups and detached crystal fragments play a secondary role in shaping the methanol isotherms. The unique combination of high adsorption capacity and low relative pressures both for adsorption and regeneration is desirable for various applications including pressure swing separations, air pollution abatement, and adsorptive heat pumps.

Introduction

In the first comprehensive study on the adsorption properties of hydrophobic surfaces, Kiselev[1] used the isotherms of H_2O, methanol, some hydrocarbons, and CCl_4 to demonstrate that an amorphous silica adsorbent loses its adsorption capacity for both polar and nonpolar adsorbates when its surface is dehydroxylated. Only weak London dispersion or van der Waals forces remain in effect on such "nonspecific" surfaces. Chen[2] pointed out that aluminum-deficient zeolites with a low hydroxyl content are crystalline, uniformly microporous, hydrophobic counterparts of the amorphous, mainly mesoporous, hydrophobic silicas. He used repeated steamings and HCl leaching to obtain hydrophobic mordenite, but numerous other aluminum reducing techniques have also been developed for various zeolites.[3,4] Leaching with NaOH,[5] H_4EDTA,[6] or oxalic acid,[7] reactions with F_2,[8] $SiCl_4$,[9] or $(NH_4)_2SiF_6$,[10] and direct synthesis from aluminum free ingredients[11] are among some of the well-known examples.

Unlike most amorphous hydrophobic silicas, hydrophobic zeolites adsorb substantial amounts of nonpolar adsorbates, such as hydrocarbons, chlorinated hydrocarbons, argon, nitrogen, oxygen, etc., at low vapor pressures (p) and reach pore volume filling below the dew point pressures (p_o) of these adsorbates.[9,11,13,14,17,18] The corresponding Type I or classic Langmuir isotherms are typical for micropore adsorption.[19−23] These isotherms commonly begin to rise at $p/p_o < 10^{-4}$ relative pressures and arrive at a nearly horizontal saturation section around $p/p_o \approx 0.01$ unless some intentional or unintentional lattice defect causes distortions, mostly toward the Type IV isotherm.[2,3,24−26] The high adsorption capacity of microporous materials at low relative pressures has long been attributed to their enhanced adsorption energy generated by the overlapping potential fields of atoms constructing the walls of narrow (<20 Å diameter) pores.[19,21,27] However, some recently discovered micropore-specific physisorption and diffusion phenomena, e.g., repulsion potential at pore entrances or curvature effects[28,29] and enhanced mobility of adsorbates having comparable dimensions to the channel size or levitation effects,[30−33] calls attention to the imperfect understanding of these systems.

Among the poorly elucidated adsorption properties of hydrophobic zeolites is their hydrophobicity itself, i.e., their reluctance to adsorb water[2,8,9,11,12,25] and certain other polar molecules such as alcohols[8,15,34−36] or NH_3.[9] One would expect that hydrogen bonds would keep these molecules associated together in the zeolite pores. In contrast, n-hexane which condenses easily does not form hydrogen bonds.[11,24] Some researchers[37−39] think that the higher polarizability of hydrocarbons versus water might be a key factor because polarizability determines the strength of cohesion between the adsorbate molecules and the nonspecific adsorbent surface.[19−21] However, this explanation cannot account for several facts including the high adsorption capacity of hydrophobic zeolites for nitrogen or argon which also have low polarizability similar to water, and their low adsorption capacity for alcohols that are much more polarizable than water or nitrogen. Carrott et al.[40−42] suggested that the low water adsorption capacity of silicalite should be due to its small approximately 5.5 Å diameter pores which "cannot easily accommodate the three-dimensional array of hydrogen bonded water molecules". Nonetheless, this explanation does not hold for hydrophobic, microporous adsorbents having $d >$ 6 Å pores including for instance, siliceous beta and Y zeolites

Similar to any hydrophobic adsorbent, hydrophobic zeolites adsorb negligible amounts of water up to about $p/p_o \approx 0.7$ relative pressures giving Type III isotherms.[19−23] Copious lattice defects, however, might cause kinks and steps in these isotherms. Mesopores for instance, can produce a transition toward Type IV isotherms,[13,25,42] and silicon or aluminum attached hydroxyls can initiate a partial distortion to Type I isotherms.[12,13,15,25,34,43,44] Because such defects may easily occur, various methods have been developed for indexing the level of hydrophobicity.[2,12,13,16,17,45]

Brunauer et al.,[20] Kiselev,[1,46,47] and Dubinin[48] called attention to a very special, but rare, isotherm change: water and methanol

* To whom correspondence should be addressed. E-mail: ihalasz@pqcorp.com.

10.1021/jp0103530 CCC: $20.00
Published on Web 10/09/2001

molecules that typically show negligible adsorption over hydrophobic carbon and silica may abruptly condense at $p/p_o < 0.7$ relative pressures. The reported explanation for this effect is that adsorbates capable of forming strong intermolecular hydrogen bonds adsorb first as isolated molecules but, with increasing surface coverage, they become associated causing an abrupt condensation.[1,20,21,32,47,48] Over microporous hydrophobic carbons[11,20,32,42,48-50] and $AlPO_4$-5 type molecular sieves,[42,51-53] the condensation of water can lead to pore volume saturation in the range of $p/p_o \approx 0.6-0.8$ and 0.2−0.4 relative pressures, respectively. It is conjectured that oxygen and hydroxyl surface contamination might contribute to this pore saturation, but it has remained unclear why the condensation pressures are so different from each other. The corresponding Type V adsorption isotherms are extremely rare.[19-23] Apart from adsorption of water over the cited two microporous adsorbents, true Type V isotherms have been only reported for water, benzene, and N_2 over mesoporous Vycor[54,55] and MCM-41[56,57] with pore saturating steps at approximately $p/p_o \approx 0.8$ and 0.2, respectively. These steps are generally attributed to hydroxyl assisted condensation in the extremely narrow ($d \approx 25$ Å) mesopores.

Neither alcohols nor zeolites have been associated with Type V isotherms before. Here we report the observation of such an isotherm for methanol adsorption on an aluminum-deficient commercial Y-zeolite, CBV-901, which is the latest member of the Y-zeolite family produced by Zeolyst International.[58] In contrast to other microporous adsorbents giving Type V isotherms, this zeolite does not adsorb substantial amounts of water up to $p/p_o \approx 0.7$, i.e., it is truly hydrophobic. It also adsorbs negligible amounts of methanol up to about $p/p_o \approx 0.1$ relative pressure, but an abrupt pore saturation occurs between p/p_o 0.1 and 0.2 relative pressures. Besides methanol adsorption isotherms, this paper presents results of various adsorption experiments and grand canonical Monte Carlo molecular simulations of the adsorption of methanol. It will be shown that the observed Type V isotherm is a genuine property of the dealuminated Y-zeolite possibly controlled by a combined effect of the pore size and the force field. Lattice defects can only play a secondary role in shaping these isotherms.

Experimental Section

Adsorbents and Adsorbates. CBV-901 is a commercial product of Zeolyst International made by a patent pending procedure[59] based on alternating thermal, hydrothermal, and acid leaching treatments. This is a well-crystallized Y-zeolite with a 24.24 Å lattice constant and a low (<0.03%) sodium and aluminum (Si/Al ≈ 40) content.

Methanol and cyclohexane vapors were generated from high purity liquids from Fluka. Water vapor was produced from deionized water. The N_2, Ar, and He gases were 99.99% or higher purity products from MG Industries.

Adsorption Measurements. All adsorption experiments were performed using a commercial RXM-100 type instrument from Advanced Scientific Designs, Inc. (ASDI). Fresh zeolite samples were used for measuring each vapor isotherm. Liquids for generating vapors were placed in fused quartz containers. Prior to vapor adsorption measurements, these containers were submerged into liquid nitrogen and the gas phase above the frozen material was evacuated to $<10^{-3}$ Pa to remove any traces of air. The freeze−thaw degassing was done a minimum of three times. A sample of <0.1 g zeolite powder was weighted into a quartz sample holder and pretreated for 2 h at $< 10^{-3}$ Pa and 500 °C to remove any adsorbed materials. To avoid lattice damage, the final temperature was reached by programmed heating at 10 °C/min with 30 min breaks at 120 °C and 200 °C. After pretreatment, the reactor was cooled under vacuum to the temperature of adsorption and known volumes of adsorbates were dosed at increasing pressures. The system pressure was equilibrated after each dose (usually 3 to 20 min was needed to reach steady state pressure), and the adsorbed amount was calculated from the pressure drop before and after the dosage. Steady state pressure was controlled by setting the slope of the pressure drop to <1 % between subsequent readings. To avoid errors associated with cold-spot condensation, the dosing manifold, valves, gauges, and reactor were carefully tempered to the adsorption temperature. The void volume in the reactor was determined by He adsorption. The micropore distribution was measured by Ar adsorption at liquid argon temperature and calculated using the equation from Saito and Foley.[29] The mesopore distribution was determined by N_2 adsorption and calculated with the BJH method.[60] The average error for adsorption measurements, including repeatability, was <±5%.

Molecular Modeling. Virtual adsorption experiments were performed using the Sorption module of CERIUS2 (versions 3 through 4.2) molecular modeling program from MSI. Sorption implements a statistical mechanics method using Metropolis Monte Carlo algorithm[61] (NVT ensemble) for calculating the isosteric heat of adsorption and Grand Canonical Monte Carlo procedure (NPT ensemble) for simulating adsorption at fixed pressure (or constant chemical potential). Pressures and temperatures were selected within the range of our experimental parameters. At these conditions, the fugacity coefficient for methanol vapors is approximately 1 thus using direct pressure values is correct. Based on preliminary model experiments, a minimum of 1×10^7 iterations were needed to reach energy equilibrium for data points in the inflection zone of the adsorption isotherms, and at least twice as many to keep standard deviation from the average energy below about ±10%. Thus, 2×10^7 iterations were used for calculating every data point around the step in the isotherm. In the initial and final linear sections, equilibration with ~±2% accuracy was typically attained after 1×10^6 iterations. These conclusions were drawn after testing the effect of virtually every parameter that the program permitted and compiling a good combination to emulate our experimental data. The selected parameters for virtual adsorption experiments are given below.

A Y-zeolite model with a 24.26 Å lattice constant was fabricated based on experimental XRD data.[62] Methanol and hexane models were made using the 3D-Sketcher routine of CERIUS2. The special N_2 and TIPS2[63] water models are provided as adsorbates in the general program package. After energy minimization, atoms of the adsorbate molecules were associated with appropriate hybridization, formal charge, aptitude for hydrogen bonds, occupancy, etc., physical and chemical properties that appear in the main Visualizer module. The partial charges of elements were calculated using the electronegativity equalization method[65] provided in the Qeq_charged1.1 program of the Charges module. These charge calculations were made with maximum 500 iterations using a convergence factor 5×10^{-4}.

The Buchart 1.01-Dreiding2.21 force field[64] was used for attributing molecular parameters for energy calculations except the partial charges and hybridization of atoms that were determined as described above. The general rules outlined by Mayo et al.[64] were followed for atom typing. An exception was the carbon atom in methanol that had to be assigned to type

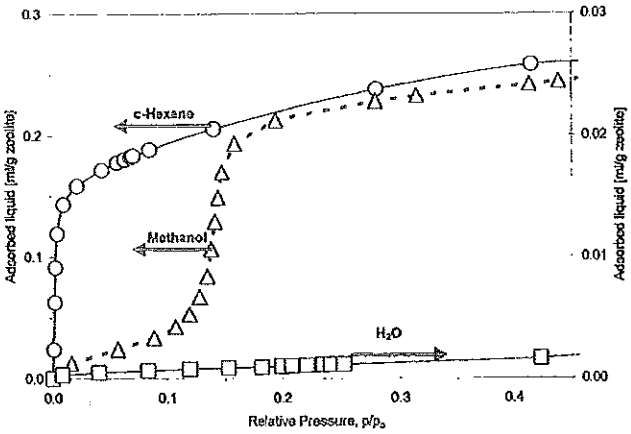

Figure 1. Adsorption of hydrophilic and hydrophobic molecules on CBV-901 at 21 ±1 °C.

C_33 (mass was reduced to 12 g/mol) while the separate type H_hydrogen atoms of the methyl group had also been kept. Bond orders were not specified and atomic motions were allowed for every molecule. All valence (13), nonbond (4), and restraint (harmonic) possibilities have been selected in the Energy Terms section of the Open Force Field (OFF) module. The Ewald[66] summation was selected for the van der Waals and Coulomb calculation preferences and the Ewald parameters were estimated using the SMART Optimization Policy. The dielectric constant was set to 1 (vacuum), the search for neighbors to SMART with minimum 1 and maximum 100 000 neighbors (the program decides automatically when the Ewald parameters are to be estimated), and the accuracy for the optimization to 4.19 J/mol. Arithmetic combination rule was selected for the van der Waals interactions. The Hydrogen Bond Preference was set to Spline with 3 to 4.5 Å and 30 to 89° spline-on and spline-off limits for the donor−acceptor distances and angles, respectively. H-bond list was not used. For every other parameter the default values were permitted in the OFF module.

In the Sorption module, 0.1 Å translation steps and 2° rotation steps were selected with an automatic re-scaling function after every 100 000 trials by a factor of 1.01. A trajectory file was generated by collecting data at every 5 000th step. The very recently released 4.2 version of Cerius2 also permits collection of snapshots about molecular arrangements at selected intervals during the run. The real space interaction cutoff distance was between 6.8 and 7.4 Å obtaining best isotherm fits with 7.3 and 6.9 Å at 20 and 60 °C, respectively. The Ewald parameters were generated automatically and 0.1 Å approaching distance was permitted for the adsorbate molecules. The typical Ewald sum constant for Met-OH at these conditions is around 2.9 Å. To reduce calculation time, model experiments were made only on one unit cell (576 atoms) of the zeolite.

The total framework potentials were calculated by entering appropriate commands manually because the automatic calculation module does not allow input of accurate *a*, *b*, *c* space point values due to a bug in the program.

Results

Vapor Adsorption Experiments. Figure 1 compares the adsorption isotherms of cyclohexane, water, and methanol on CBV− 901 at room temperature. As expected, this hydrophobic Y-zeolite adsorbed very low amounts of water up to $p/p_o \approx 0.7$ relative pressure (Figure 1 shows values at $p/p_o < 0.5$ for better visibility). Measurements at higher pressures were not made due to errors caused by wall condensation. The hydrophobic cyclohexane shows a Type I adsorption isotherm, typical for micropore adsorption. The sorptive capacity for both water and the hydrocarbon agrees well with data published for various dealuminated faujasites.[3,6,9] Consequently, the structure of CBV-901 is similar to the typical hydrophobic Y-zeolite structures.

Because the adsorption of alcohols generally requires similar hydrophilic surfaces as that of water, it was surprising to observe a substantial methanol uptake above $p/p_o \approx 0.1$ after an initial low adsorption (Figure 1). This is a rare Type V adsorption isotherm[20−24] with a step at an unusually low relative pressure. The closest experimental example with a sharp upswing beginning at around $p/p_o \approx 0.2$ relative pressure has been reported for the adsorption of H_2O on $AlPO_4$-5 type molecular sieves.[42,52,53]

Figure 1 indicates that the pore volume filling with methanol is about the same as that with the cyclohexane therefore, the Gurevits rule[21] is obeyed. The so-called kinetic diameter,[11,67] i.e., the spherical diameter of molecules calculated from the covalent radii of composing elements, is about 3.8 Å for methanol and 5.7 Å for cyclohexane. Thus, there is no possibility for close hexagonal packing in the 7.4 Å average diameter channels of the Y-zeolite even when the adsorbate molecules can touch each other, which is highly unlikely. If the pore filling involves liquidlike condensation as is generally accepted in the adsorption literature and gives the basis for the Gurevits rule,[21,23] each liquid phase methanol and cyclohexane molecule should occupy approximately a 5.1 and a 7 Å diameter sphere, respectively. For these methanol and cyclohexane sizes, the total accessible volumes in a perfect, aluminum free Y structure with a 24.26 Å lattice constant are 5932 and 4484 Å^3/unit cell (UC), respectively. Consequently, the theoretical maximum for this zeolite is the accommodation of 88 molecules/UC or 0.31 mL/g of liquid methanol and 25 molecules/UC or 0.23 mL/g of liquid cyclohexane provided the condensed adsorbates can continuously fill the total available volume. Two 7 Å diameter spheres cannot fit into the 13 Å diameter supercage, and only six 5.1 Å diameter spheres can be placed into one of these cavities. Thus, there is obviously no continuous space filling with these liquidlike molecules in the micropores of a Y-zeolite. A broad analysis of similar situations in cylindrical and slit shaped micropores lead Carrot and Sing[40] to calculate the degree of packing for different adsorbate/pore opening ratios. Using their estimates, the degree of packing for methanol is about 64% which results in 56.3 (= 0.64 × 88) molecules/UC or 0.20 (= 0.64 × 0.31) mL/g zeolite in good agreement with the experimental values (Figure 1). The same numbers for cyclohexane are 42%, 10.5 (= 0.42 × 25) molecules/UC or 0.11 (= 0.42 × 0.23) mL/g zeolite. It is not clear at this time why these numbers are much lower than the experimental cyclohexane adsorption (Figure 1). A possibility is solidlike adsorption similar to that suggested for N_2[68] and *n*-heptane[69] over the ZSM-5 type silicalite.

The odd isotherm shape for methanol was repeatedly observed at many temperatures between 0 and 80 °C. Note that full pore volume filling above 60 °C has not been reached due to the technical limits (cold-spot exclusion) of our instrument. The total adsorption capacity at 0 °C (~0. 23 mL/g at $p/p_o = 0.3$) was reduced by about 25% at 60 °C, which is indicative of the lack of formation of a true liquid phase in the micropores (liquid volumes are less sensitive to temperature changes). However, the adsorption of methanol over CBV-901 is true physisorption as determined from more than 1500 adsorption−desorption cycles between 20 °C and 175 °C without significant performance changes.[70]

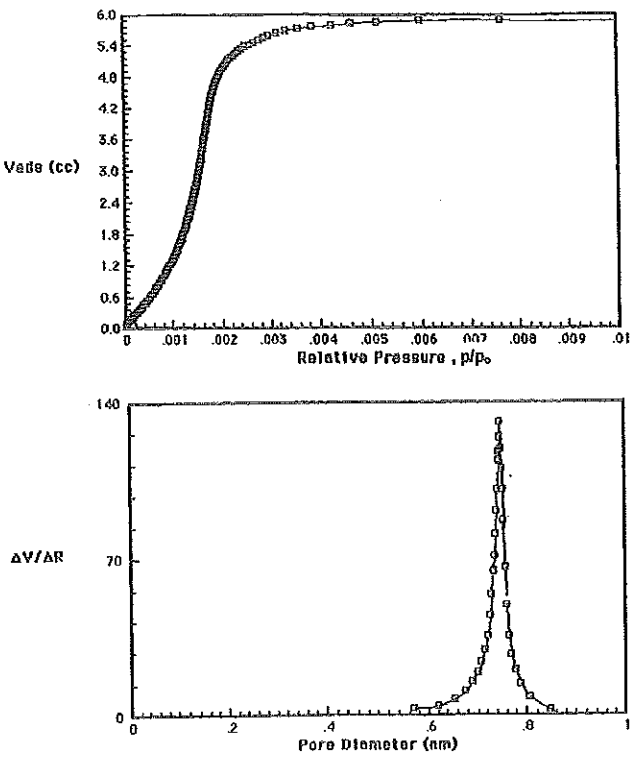

Figure 2. (a) Adsorption of Ar on CBV-901 (0.0558 g) at 87 K; Vads (cc) = adsorbed mL gas calculated at STP conditions; after pore saturation at $p/p_o = 0.01$ the adsorbed Ar corresponds to 0.13 mL liquid/g zeolite; (b) micropore size distribution calculated using the SF method.[29]

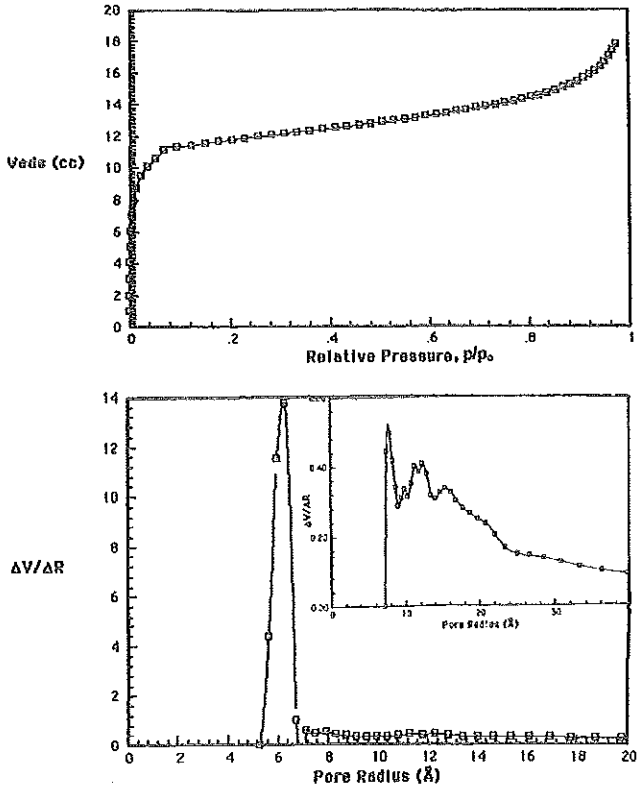

Figure 3. (a) Adsorption of N_2 on CBV-901 (0.0558 g) at 77 K; Vads (cc) = adsorbed mL gas calculated at STP conditions; after pore saturation at $p/p_o = 0.1$ the adsorbed N_2 corresponds to 0.31 mL liquid/g zeolite; (b) mesopore size distribution calculated using the BJH method;[60] insert magnifies the range of less significant pores.

The selectivity of aluminum deficient faujasites for adsorbing alcohols over water has been studied before, but only about 10% pore filling was attained when hydrophobic (Si/Al > 20) samples were tested.[35,36] Type V adsorption isotherms have not been reported over zeolites, and the adsorption of methanol on CBV-901 is the first example of such an isotherm with alcohols. Thus, we speculated about the possible causes of this unique finding. This zeolite is not totally aluminum free (nominal SiO_2/Al_2O_3 ratio is ~80). Its complex synthesis procedure can generate a variety of defects such as formation of mesopores, bridging hydroxyls, incompletely removed silanol groups, pore blocking by detached lattice fragments, and extra lattice AlO_x species, and they were among the factors considered first. Porosity measurements and molecular modeling experiments were performed to see the potential role of these parameters.

Porosity Measurements. The micropore distribution of CBV-901 was measured by Ar adsorption from about $p/p_o \approx 10^{-7}$ to 10^{-2} relative pressures. Figure 2 shows the typical Type I isotherm for Ar, and the calculated pore distribution. From the single maximum near 7.5 Å it appears that only the typical Y zeolite channels are present in this sample. Formation of other micropores via lattice atom removal or pore plugging was not measurable in the pore diameter range from about 4 to 10 Å.

Figure 3 shows the results of mesopore measurements with N_2. The slope in the saturating section ($p/p_o > 0.1$) of the isotherm in Figure 3/a is somewhat less steep, and the adsorption capacity is somewhat higher than that usually reported for aluminum deficient zeolites.[3,18] These values are closer to data typical for the mesopore-free, nondealuminated Na−Y zeolites.[3,18,67] The adsorbed liquid N_2 volume is about 0.31 mL/g zeolite which is larger than the average 0.24 mL/g zeolite obtained with cyclohexane and methanol (Figure 1). Considering the above-mentioned gaslike response of adsorption volume on temperature, the big N_2 adsorption capacity might be due to the low temperature of adsorption.

As one could expect from the shape of the N_2 isotherm, the only significant pore size maximum in the range from $r = 5$ to 200 Å was at $r = 6.3$ Å or $d = 12.6$ Å which corresponds to the typical supercage diameter in Y-zeolites (Figure 3/b; only the range $r < 20$ Å is shown for better clarity). The insert in Figure 3/b magnifies the pore distribution after subtracting the zeolite micropores with $r < 7$ Å radii. The three major peak maxima correspond to pores with $d = 15.9$, 24.7, and 30.8 Å diameter. Figure 4 illustrates that at least two of these extreme narrow mesopores can form by destroying bridges separating the big cavities (supercages) of the faujasite crystal. However, Figure 3 clearly indicates that the relative amount of these enlarged pores is negligible and hence cannot substantially influence the shape of methanol isotherm.

Virtual Adsorption Experiments with Model Molecules. To exclude the potential effect of various lattice defects on the adsorption of methanol, virtual adsorption experiments were performed on a defect-free dealuminated Y-zeolite at the same conditions as in the real experiments on CBV-901. Despite a large number of model studies with methanol and Y-zeolite, model adsorption isotherms with this adsorbent−adsorbate pair have not been published.

Figure 5 compares the results of the real and virtual adsorption experiments with methanol at two different temperatures. The models simulate the real isotherms remarkably well. Only the higher saturation limit is different from the real value, which is understandable considering that we do not have a program for correcting a nonrealistic force field generated ion size for the zeolite (the force field uses van der Waals atom radii), and the

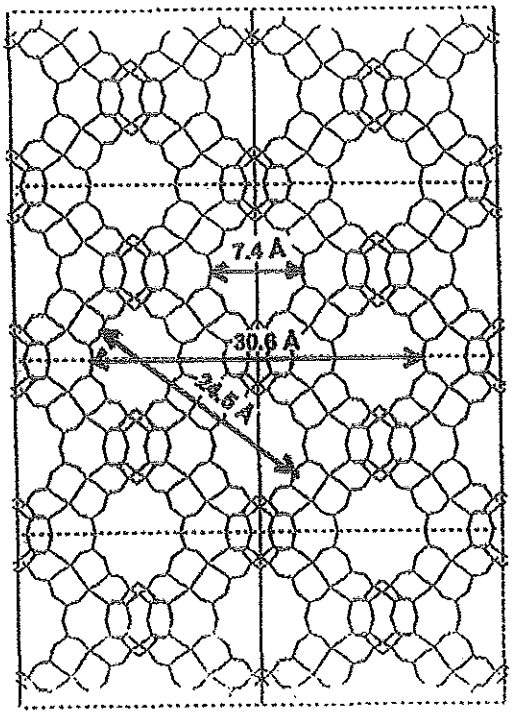

Figure 4. Typical dimensions in the aluminum free Y-zeolite lattice (111 view).

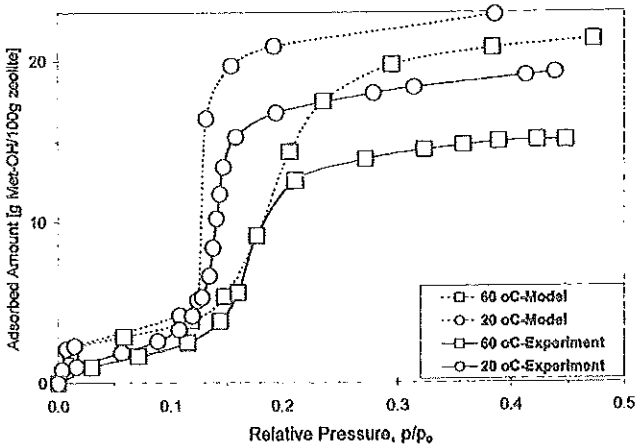

Figure 5. Simulated (dashed lines) and experimental (continuous lines) adsorption isotherms for methanol on CBV-901 at 20 °C (circles) and 60 °C (squares).

model cannot take into account the real space requirement of condensed molecules that were discussed above.

The close match of the real and virtual adsorption curves indicates that they are inherently connected to the aluminum-free Y-zeolite structure and any defect in the real Y-structure can only have a secondary effect on the methanol isotherm. We probed the reality of our zeolite model by adsorbing water which gave a realistic Type I adsorption isotherm in virtual adsorption experiments over a Na-X zeolite. Similar to the real CBV-901, water did not adsorb on our model Y-zeolite. We also made comparative experiments with our methanol model over ZSM-5 silicalite and found Type I isotherms in agreement with experimental reports.[71−73] Thus, one can conclude that results of these virtual experiments reflect real events. It is important to note, however, that the virtual adsorption runs with methanol over the siliceous Y-zeolite only fit the experimental

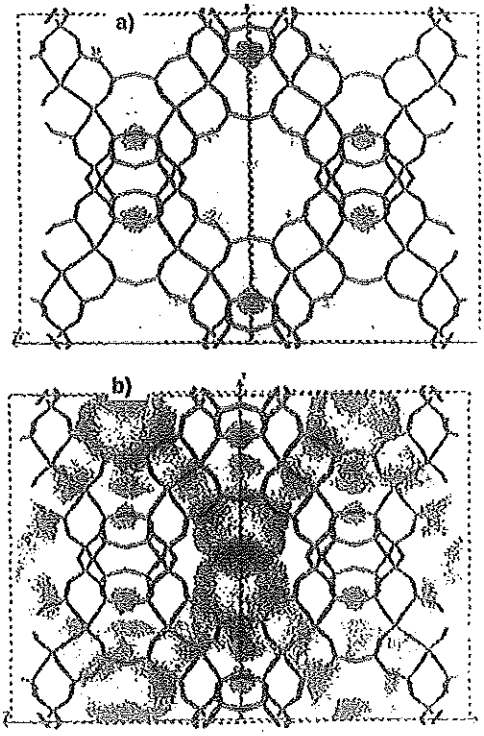

Figure 6. Mass dispersion map of methanol in the zeolite framework (111 view) at $p/p_o = 0.11$ (a) and $p/p_o = 0.18$ (b) relative pressures; grand canonical Monte Carlo simulations at 25 °C after 2×10^7 cycles. The light gray four-connected atoms in the lattice represent Si^{4+} cations; the dark lines are O^{2-} anions; the tiny gray spots accumulated into patches show the statistical distribution of the mass centers of methanol molecules at energy minima; the darker are the patches the higher is the probability that adsorbed methanol resides in the given area. Note that methanol molecules adsorb mainly between Type II* and Type III′ positions (see Figure 7) at low pressure (a) and these molecules are not connected to the other molecules filling up the supercages at high pressure (b).

data on CBV-901 when the distance of molecular interactions is limited to a narrow, 6.8−7.3 Å range that corresponds to the three-dimensional pore opening of faujasite.

Figure 6, parts a and b, shows respectively the typical distribution of methanol molecules at the beginning and the top of the sharp step in the adsorption isotherm. Clearly, the low-pressure adsorption that corresponds to <2 molecules per supercage (<4.5 g MetOH/100 g zeolite, Figure 5) is restricted to a location between the Type II* and Type III′ positions of the zeolite[67,74,75] (Figure 6/a). These positions within the supercage are in front of a square face of the hexagonal prisms interconnecting the sodalite units (Figure 7). It is noteworthy that the adsorption position of methanol in this aluminum free Y zeolite coincides with the adsorption position of water in alkaline exchanged X zeolites.[75] This finding suggests that the lattice potential might determine the adsorption of polar molecules in this position regardless of the surrounding exchangeable ion environment. Although this issue has yet to be probed in comparative model calculations, we found that the average potential at these positions is -35 ± 10 kJ/mol versus the average -95 ± 20 kJ/mol value at most other places in the main channels and cavities of the zeolite (vide infra).

Figure 6b indicates that the first adsorbed methanol molecules do not participate in the condensation at high pressures where the condensed methanol molecules form a regulated network connected through the supercage windows. Distance measurements suggest that the center of the oxygen atoms of these latter methanol molecules are in closer average proximity to each other

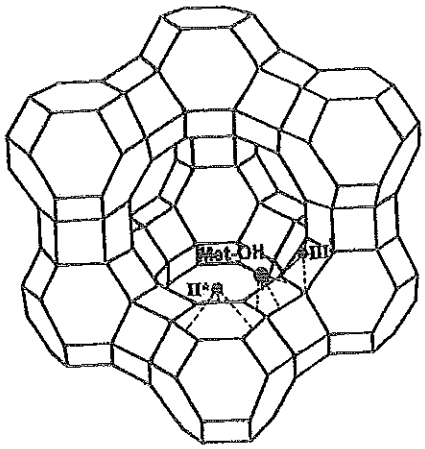

Figure 7. Structural scheme of the Y zeolite indicating the main location of methanol molecules adsorbing at low pressures (see also Figure 6a).

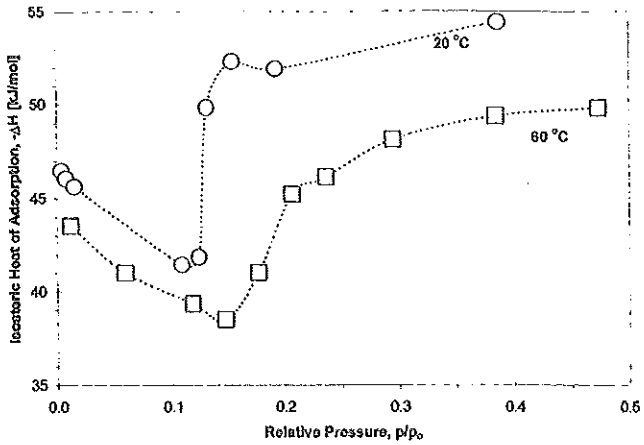

Figure 8. Calculated adsorption enthalpies for methanol over a dealuminated Y-zeolite model. Results were computed after reaching adsorption equilibrium at a given pressure and temperature. Note that the upswing represents heat of condensation evolving during micropore filling.

(~4 Å) than to the center of oxygens in molecules adsorbed first (~8 Å). Note, however, that these distances vary by ±1 Å or more and the radius of oxygen is around 1.4 Å, thus the surfaces of oxygen atoms are by about 2.8 Å closer to each other than their centers. Because the model permanently translates, rotates, adds, and eliminates adsorbate molecules and the distances between the molecules are relatively large, the orientation of molecules has dubious physical meaning hence have not been evaluated. The ~4 Å average distance of condensed species approximates a typical H-bond length. The program implicitly calculates hydrogen bonds, but the explicit existence of these bonds cannot be visualized and proved by the model. The energy analysis of the system before and after methanol adsorption at 25 °C and 1800 Pa shows substantial increase in the large electrostatic (from $\sim -6.2 \times 10^3$ kJ/mol to $\sim -6.6 \times 10^4$ kJ/mol) and moderate increase in the smaller van der Waals (from $\sim 5.0 \times 10^2$ kJ/mol to $\sim 8.9 \times 10^2$ kJ/mol) energies among the nonbond energy terms that affect the adsorption process. However, hydrogen bond energies did not appear among the nonbond energy terms despite assigning hydrogen-bond donor and acceptor properties to the methanol hydroxyls. The reasons are not clear at this time.

Both manual distance measurements and results from radial atom distribution function analysis (RDF) indicate that the span between the oxygen centers of methanol molecules and the centers of the closest lattice oxygen atoms varies from 3.5 Å to about 8 Å with roughly equal probability. Consequently, most adsorbate molecules are in closer proximity to each other than to the lattice atoms. This observation suggests (but does not prove in lack of proper hydrogen bond and interaction energy analysis for which we are not equipped) that strong adsorbate–adsorbate interactions might be more important for the condensation than the direct interaction between the methanol molecules and the zeolite atoms. In agreement with this conclusion, Figure 8 shows that the heat of adsorption decreases as fewer and fewer adsorption sites remain free on the surface of zeolite but suddenly increases when the heat of condensation (~35.2 kJ/mol at 25 °C[76]) is approached. That step coincides with the abrupt increase in the adsorption isotherms (Figure 5). The range of calculated adsorption heats agrees well with published experimental data for methanol adsorption over aluminum deficient Y-zeolite.[77]

In an effort to explain the different methanol adsorption isotherms on the siliceous Y and ZSM-5 zeolites, we calculated the lattice potentials that an adsorbate molecule "feels" when moving in the micropores of these zeolites. Substantial variations were measured at various positions in both zeolites. At certain positions even a slight, 1 or 2 Å, difference in the space can cause substantial potential change. For example, moving toward the III′ position from the above-mentioned adsorption position of "spectator" methanol molecules (Figures 6a and 7) causes a potential change from about −35 kJ/mol to −100 kJ/mol and moving toward the center of the square face of the closest hexagonal prism leads to a total potential of about 75 kJ/mol (note that the negative and positive potentials are mainly associated with negative and positive electrostatic charges). The potential changes are generally sharper near the surface atoms than in the large cavities probably because the equilibrated Coulomb potential of the large negative oxygen ions dominates at larger distances from the surface but the small positive silicon ions also gain significance at proper positions in shorter distances together with the short range van der Waals forces. Because micropore condensation typically occurs in the main channels of zeolites and little is known about the longitudinal potential deviations along these channels, we measured the total potentials at the center of the channels across the unit cells of the siliceous ZSM-5 and Y zeolites.

One curve in Figure 9a shows slight but characteristic fluctuations around an average −95 kJ/mol potential in the center of Y zeolite pores. The other curve in Figure 9a (dashed line) shows that the adsorption of methanol at 1500 Pa and 25 °C causes only minor potential changes at the same points. The potential minima are in the centers of the 12 member windows of supercages and the potential maxima correspond to the middle of supercages (but not to their geometric center which is in a different space position). Note that nowhere does the negative potential drop to $> -35 \pm 10$ kJ/mol that is the average value in the positions for methanol adsorption at low pressures (Figures 6a and 7). It is reasonable to assume that at more negative potentials the adsorbent–adsorbate attraction is not strong enough to overcome the Coulomb repulsion toward the negatively charged large hydroxyl heads of methanol molecules. Diagonal measurements across a supercage window indicate minor potential changes compared to that in the center point except in the close proximity (>3 Å from the center) to the surface of lattice oxygens where the negative potential increases substantially (← 130 kJ/mol). Yashonath and Santikary[30] found similar longitudinal potential fluctuations as shown in Figure

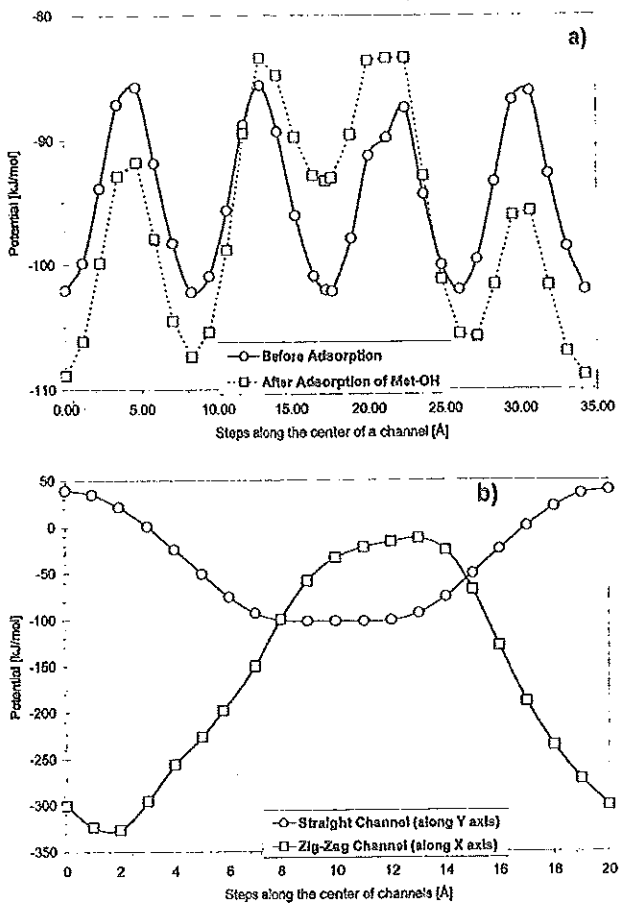

Figure 9. Variations in the total (electrostatic plus van der Waals) potential that an adsorbate molecule senses when flying along the center of the microchannels of aluminum free Y (a) and ZSM-5 (b) zeolites. The potentials in the unit cell of Y zeolite (a) were calculated between points 0.5, 0, 0 and 0.5, 1, 1 before and after adsorption of methanol at 25 °C and 1500 Pa. The potentials in the unit cell of ZSM-5 (b) were calculated along the channels beginning at points 0, 0.25, 0.38 (sinusoid channel) and 0.5, 0, 0.5 (straight channel).

9/a and suggested that these fluctuations were responsible for the levitating effect observed during the diffusion of certain molecules.

In contrast to the Y zeolite, the center of the ZSM-5 micropores shows substantial longitudinal potential deviations (Figure 9/b). At the crossing of the well-known perpendicular sinusoid and straight channels (where the two potential curves cross each other in Figure 9/b) the potential is similar to the average potential measured in the Y channels (Figure 9/a), but large negative and positive deviations occur at other points. Consequently, there are numerous positions, even in the center of ZSM-5 channels, that offer $>-35 \pm 10$ kJ/mol potential for the adsorption of methanol that results in a Type I adsorption isotherm. The large longitudinal potential variation in ZSM-5 is presumably due to the relatively small distance between the center of the channels and the pore wall atoms. In the sinusoidal channels, for instance, the average free pore diameter is as low as ~4 Å (along a straight center line and measured from oxygen surface to oxygen surface). This distance is almost half of that in the Y channels hence the effect of van der Waals forces and silicon ions on the adsorbate molecules is more significant in ZSM-5 than in Y. The potential differences in the pores of Y and ZSM-5 zeolites fit to the reported experimental differences in the adsorption properties of "narrow" and "large" micropore materials[40,42] as outlined later in this paper.

Discussion

In their milestone paper, Brunauer, Deming, Deming, and Teller[20] recognized the Type V isotherm as a separate category of isotherms based on a single instance of water adsorption on charcoal observed by Coolidge[78,79] in the nineteen twenties. In 1985, the IUPAC classification of isotherms noted only that "The Type V isotherm is uncommon: it is related to the Type III isotherm in that the adsorbent–adsorbate interaction is weak, but is obtained with certain porous adsorbents".[22] Besides the water–carbon system, only the water-$AlPO_4$-5[42,51–53] system has been found to give true Type V isotherms involving microporous adsorbents. These latter isotherms are especially interesting because their step begins at a very low, $p/p_o \approx 0.2$, relative pressure which excludes a mesopore-type capillary condensation that would require $p/p_o > 0.4$ relative pressures.[21]

Studies on water isotherms over carbon and $AlPO_4$-5 were instrumental in recognizing that "micropore-filling" does not involve the initial monolayer building and growing adsorbate layer on the pore walls that cause condensation in mesopores.[40–42] It became increasingly clear that only the adsorption in narrow micropores might involve significant adsorbent–adsorbate interactions leading to pore saturation at $p/p_o < 0.01$ relative pressures. Adsorbate–adsorbate interactions dominate in larger micropores ($d < 20$ Å) and cause micropore filling even without the involvement of surface atoms at $p/p_o > 0.02$ relative pressures.[32,40–42] In this respect, "large" and "narrow" have not necessarily been defined because the ratio of pore opening/molecular diameter] seems to be important, not the absolute size of the micropores.[30,40]

These decade old findings however have still not found a widespread acceptance largely because they are based on the confusing adsorption of water, which is a special adsorbate.[21,32,42,50] Abandoning the conviction that hydrophilic surface sites must contribute to the adsorption of water seems to be difficult. Until recently, oxygen contamination was frequently assumed when water or alcohol adsorption was observed over microporous carbon,[32,50] and hydroxyl contamination was assumed on the oxygen-paved surface of $AlPO_4$-5 to explain water adsorption.[42,53] The role of these sites remains dubious. An interesting example for micropore condensation without hydrophilic surface sites could be the reported Type I adsorption isotherms of alcohols over truly hydrophobic ZSM-5 type silicalite.[71–73] However, this zeolite belongs to the group of "narrow" micropores that preferably attract adsorbates via van der Waals forces. The preferred role of adsorbate–adsorbate interactions over adsorbent–adsorbate interactions in the micropore condensation process is not well supported. Moreover, the inability of this zeolite to adsorb water was explained by geometric restrictions in accommodating three-dimensional water arrays[40–42] not with the lack of hydrophilic surface sites. Thus, a pure example for the adsorbate–adsorbate interaction controlled micropore condensation in "large" micropore adsorbents has been missing.

The Type V adsorption isotherm of methanol over CBV-901 fills this gap. This truly hydrophobic microporous adsorbent has large, ~7.4 Å diameter, pore openings leading into ~13 Å diameter cages.

The early upswing in the Type V adsorption isotherm (Figures 1 and 5) cannot be associated with hydrophilic defects otherwise water should adsorb even better than methanol. There is ample proof in the literature that methanol can form hydrogen bonds.[80–82] Apparently these hydrogen bonds can contribute to keeping the methanol molecules together once the relative pressure exceeds the critical $p/p_o \approx 0.1$ energy level. The

comparison of Figure 6, parts a and b, clearly indicates that adsorbate−adsorbate interactions determine the formation of condensed methanol arrays at $p/p_o > 0.1$. These condensed molecules (Figure 6b) are closer to each other than to the surface atoms and have literally no connection to the first few molecules attracted by dispersion forces to the faujasite lattice at $p/p_o < 0.1$ (Figure 6a). Atoms around this position are facing the entrance of the supercages (Figure 7); thus, they are presumably least affected by the potential field of the opposing pore wall which manifests itself in the low negative potential (~−35 kJ/mol) in this area. The abrupt heat increase in Figure 8 reflects the condensation heat as Kiselev[1,46,47] described.

Thus, the adsorption of methanol on hydrophobic Y-zeolite proves that micropore-filling in large micropores can proceed without initial island[32] or monolayer[1,21,46−48,57] building from the adsorbates around suitable active sites. Two questions, however, still remained unanswered. Why does methanol adsorb on this zeolite and water does not? Why does the methanol isotherm have a step instead of the conventional Type I or Type III shapes typical for microporous and hydrophobic adsorbents, respectively? In an attempt to answer these questions, the first thing to check is the polarizability of adsorbates.[37−39] Indeed, the higher polarizability of methanol ($\alpha_{Met-OH} \approx 3 \times 10^{-24}$ cm^3) compared to that of water ($\alpha_{H_2O} \approx 1.5 \times 10^{-24}$ cm^3) seems to answer the first question. The most polarizable c-hexane ($\alpha_{c-Hex} \approx 11 \times 10^{-24}$ cm^3) adsorbs easiest among these three molecules (Figure 1) and our model experiments also indicated some van der Waals interaction for methanol with the zeolite surface at low pressures (Figure 6a). However, we just proved that the micropore filling with methanol at higher pressures is not related to the surface sites, and it is known that the hydrogen bonds of water would easily override the polarization forces between methanol molecules. Moreover, the polarizability of N_2 ($\alpha_{N_2} \approx 1.7 \times 10^{-24}$ cm^3) and Ar ($\alpha_{Ar} \approx 1.6 \times 10^{-24}$ cm^3) are close to that of water but these molecules adsorb significantly better than water or even methanol. Further, there is no reason to assume that the polarizability of methanol increases with increasing pressure and thus, the second question remains unanswered.

It appears, however, that both questions can be answered simply by the energy barrier at the pore entrance effect elucidated by Derouane et al.[28,83,84] that give negative potential minima in Figure 9a. This potential is also known as curvature effect because it depends on the relative size of the pore opening and the adsorbate molecules in good agreement with conclusions from other calculations.[30,32,40−42] Because the siliceous Y-zeolite pores are covered with oxygen ions with negative partial charges, their repulsive force field might prevent the penetration of water molecules that have high dielectric constant ($\epsilon_{H_2O} \approx 80$) and a negative partial charge on oxygen ($\delta_O \approx -0.6$). The lower dielectric constant and oxygen partial charge of methanol ($\epsilon_{MetOH} \approx 33$; $\delta_O \approx -0.3$) would permit an easier penetration into the zeolite pores, but these molecules still have to overcome considerable repulsion. Only a few fast methanol molecules are able to slip through the energy window at low pressures. At $p/p_o > 0.1$, their concentration should be enough for virtually breaking through the energy barrier, i.e., for forming a three-dimensional array throughout the zeolite channels. The nonpolar cyclohexane, N_2, and Ar molecules ($\epsilon_{c-Hex} \approx 2$; $\epsilon_{N2} \approx 1.5$; $\epsilon_{Ar} \approx 1.3$) find little resistance thus easily entering the micropores at low pressures. When aluminum and associated exchange ions disturb the homogeneous potential field of the zeolite cavity, water will also be able to enter, and the zeolite becomes hydrophilic. In conclusion, all major experimental findings presented in this paper can be interpreted without contradiction if the force field of micropores and the dipole moments of adsorbates are considered to be as important for controlling micropore adsorption as the widely discussed pore/adsorbate geometry or the polarizability dependent induced dipole moment (van der Waals force). This conclusion also holds for ZSM-5 type silicalite that might not repel water molecules as strongly as the Y zeolite (Figure 9) but has too narrow channels for building three-dimensional arrays of hydrogen bonded water molecules without the help of surface hydroxyls.[42]

Beside the increased capacity for separating alcohols or other organic materials from water,[13,17,35,36,44] zeolite based adsorption systems with Type V isotherms can be advantageous for other applications. It has been shown, for example, that CBV-901 and methanol are better in low temperature heat pumps than any other adsorbent/adsorbate system.[70] Adsorption systems with Type V isotherms also permit adsorption and regeneration within a narrow temperature or pressure range which can be beneficial for pressure or temperature swing adsorption procedures.[39,85] Finding Type V isotherms for various organic molecules can be predictive for numerous environmental and petrochemical procedures.

References and Notes

(1) Kiselev, A. V. *J. Colloid Interface Sci.* **1968**, *28*, 430.
(2) Chen, N. Y. *J. Phys. Chem.* **1976**, *80*, 60.
(3) Scherzer, J. *A. C. S. Symp. Ser.* **1984**, *248*, 157.
(4) Szostak, R. *Stud. Surf. Sci. Catal.* **1991**, *58*, 153.
(5) Kerr, G. *J. Phys. Chem.* **1967**, *71*, 4155.
(6) Kerr, G. *J. Phys. Chem.* **1968**, *72*, 2594.
(7) Apelian, M. R.; Fung, A. S.; Kennedy, G. J.; Degnan, T. F. *J. Phys. Chem.* **1996**, *100*, 16 577.
(8) Lok, B. M.; Gortsema, F. P.; Messina, C. A.; Rastelli, H.; Izod, T. P. J. *ACS Symp. Ser.* **1983**, *218*, 41.
(9) Beyer, H. K.; Belenykaja, I. *Stud. Surf. Sci. Catal.* **1980**, *5*, 203.
(10) Parikh, P. A.; Subrahmanyam, N.; Bhat, Y. S.; Halgeri, A. B. *J. Mol. Catal.* **1994**, *88*, 85.
(11) Flanigen, E. M.; Bennett, J. M.; Grose, R. W.; Cohen, J. P.; Patton, R. L.; Kirchner, R. M.; Smith, J. V. *Nature* **1978**, *271*, 512.
(12) Olson, D. H.; Haag, W. O.; Borghard, W. S. *Microporous and Mesoporous Materials* **2000**, *35−36*, 435.
(13) Giaya, A.; Thompson, R. W.; Denkewicz, R., Jr. *Microporous and Mesoporous Materials* **2000**, *40*, 205.
(14) Von Lohse, U.; Alsdorf, E.; Stach, H. *Z. Anorg. Allg. Chem.* **1978**, *447*, 64.
(15) Nakamoto, H.; Takahashi, H. *Zeolites* **1982**, *2*, 67.
(16) Anderson, M. W.; Klinowski, J. *J. Chem. Soc., Faraday Trans. 1.* **1986**, *82*, 1449.
(17) Weitkamp, J.; Kleinschmit, P.; Kiss, A.; Berke, C. H. *Proc. 9th Intern. Zeolite Conf., Montreal, 1992;* Ed. by R. von Ballmoos et al.; Butterworth-Heinemann div. Reed Publishing Co., **1993**, 79.
(18) Schuster, C.; Hörderich, W. F. *Catal. Today* **2000**, *60*, 193.
(19) Polanyi, M. *Trans. Faraday. Soc.* **1932**, *28*, 316.
(20) Brunauer, S.; Deming, L. S.; Deming, W. E.; Teller, E. *J. Am. Chem. Soc.* **1940**, *62*, 1723
(21) Gregg, S. J.; Sing, K. S. W. *Adsorption, Surface Area and Porosity*; Acad. Press: London, *1982*.
(22) Sing, K. S. W.; Everett, D. H.; Haul, R. A. W.; Moscou, L.; Pierotti, R. A.; Rouquerol, J.; Siemieniewska, T. *Pure Appl. Chem.* **1985**, *57*, 603.
(23) Webb, P. A.; Orr, C. *Analytical Methods in Fine Particle Technology*; Micromeritics: Norcross, USA, 1997.
(24) Von Lohse, U.; Stach, H.; Thamm, H.; Schirmer, W.; Isirikjan, A. A.; Regent, N. I.; Dubinin, M. M. *Z.Anorg. Allg. Chem.* **1980**, *460*, 179.
(25) Simonot-Grange, M. H.; Elm'chauri, A.; Nafis, M.; Weber, G.; Dufresne, P.; Raatz, F.; Joly, J. F. *Stud. Surf. Sci. Catal.* **1991**, *62*, 565.
(26) Ajot, H.; Joly, J. F.; Lynch, J.; Raatz, F.; Caullet, P. *Stud. Surf. Sci. Catal.* **1991**, *62*, 583.
(27) Nguyen, C.; Do, D. D. *J. Phys. Chem.* **1999**, *103*, 6900.
(28) Derouane, E. G.; Andre, J.-M.; Lucas, A. A. *J. Catal.* **1988**, *110*, 53.
(29) Saito, S.; Foley, H. C. *AIChE J.* **1991**, *37*, 429.
(30) Yashonath, S.; Santikary, P. *J. Phys. Chem.* **1994**, *98*, 6368.
(31) Bandyopadhyay, S.; Yashonath, S. *J. Phys. Chem.* **1995**, *99*, 4286.
(32) Müller, E. A.; Rull, L. F.; Vega, L. F.; Gubbins, K. E. *J. Phys. Chem.* **1996**, *100*, 1189.
(33) Kar, S.; Chakravarty, C. *J. Phys. Chem. B.* **2000**, *104*, 709.

(34) Doelle, H.-J.; Heering, J.; Riekert, L.; Marosi, L. *J. Catal.* **1981**, *71*, 27.
(35) Weitkamp, J.; Ernst, S.; Günzel, B.; Deckwer, W.-D. *Zeolites*, **1991**, *11*, 314.
(36) Meininghous, C. K. W.; Prins, R. *Micropor. Mesopor. Mater.* **2000**, *35*−*36*, 349.
(37) Barton, S. S.; Evans, M. J. B.; Holland, J.; Koresh, J. E. *Carbon* **1984**, *22*, 265.
(38) Kiselev, A. V.; Lopatkin, A. A.; Shulga, A. A. *Zeolites* **1985**, *5*, 261.
(39) Ruthven, D. M. *Chem. Eng. Progress*. **1988**, *February*, 42.
(40) Carrott, P. J. M.; Sing, K. S. W. *Stud. Surf. Sci. Catal.* **1988**, *39*, 77.
(41) Sing, K. S. W. *Stud. Surf. Sci. Catal.* **1991**, *62*, 1.
(42) Carrott, P. J. M.; Kenny, M. B.; Roberts, R. A.; Sing, K. S. W.; Theocharis, C. R. *Stud. Surf. Sci. Catal.* **1991**, *62*, 685.
(43) Sano, T.; Kasuno, T.; Takeda, K.; Arazaki, S.; Kawakami, Y. *Stud. Surf. Sci. Catal.* **1997**, *105*, 1771.
(44) Sano, T.; Hasegawa, M.; Ejiri, S.; Kawakami, Y.; Yanagishita, H. *Micropor. Mater.* **1995**, *5*, 179.
(45) Weitkamp, J.; Ernst, S.; Roland, E.; Thiele, G. F. *Stud. Surf. Sci. Catal.* **1997**, *105*, 763.
(46) Kiselev, A. V. *Discuss. Faraday Soc*. **1965**, *40*, 205.
(47) Kiselev, A. V. In *Advances in Chromatography*; Giddings, J. C., Keller, R. A., Eds.; Marcel Dekker Inc.: New York, 1967, *4*, 113.
(48) Dubinin, M. M. In *Chemistry and Physics of Carbon*; Walker, Jr., P. L., Ed.; Marcel Dekker Inc.: New York, 1966, *2*, 51.
(49) Kaneko, K. *Stud. Surf. Sci. Catal.* **1996**, *99*, 573.
(50) Lopez-Ramón, M. V.; Stoeckli, F.; Moreno-Castilla, C.; Carrasco-Marín, F. *Langmuir* **2000**, *16*, 5967.
(51) Wilson, S. T.; Lok, B. M.; Messina, C. A.; Cannan, T. R.; Flanigen, E. M. *ACS Symp. Ser.* **1983**, *218*, 79.
(52) Theocharis, C. R.; Gelsthorpe, M. R. *Stud. Surf. Sci. Catal.* **1988**, *39*, 541.
(53) Kornatowski, J.; Rozdanowski, M. *Proc. 12th Intern. Zeolite Conf., Baltimore 1998*, USA.; Treacy, M. M. J., Marcus, B. K., Bisher, M. E., Higgins, J. B., Eds.; Materials Research Society: Warrendale, Pennsylvania, 1999, 285.
(54) Ferguson, B. C.; Wade, W. H. *J. Colloid Interface Sci.* **1967**, *24*, 366.
(55) Jones, B. R.; Wade, W. H. *Hydrophobic Surfaces, Kendall Award Symp. 1968.*; Fowkes, F. M., Ed.; Academic Press: New York, 1969, *5*, 73.
(56) Long, Y.; Xu, T.; Sun, Y.; Dong, W. *Langmuir* **1998**, *14*, 6173.
(57) Kovalenko, A. S.; Korchev, A. S.; Chernenko, J. V.; Il'in, V. G.; Filippov, A. P. *Ads. Sci. Technol.* **1999**, *17*, 245.
(58) www.zeolyst.com.
(59) Cormier, W.; Hertzenberg, E.; Cooper, D.; Marcus, B. K.; Hinchey, R. *US Patent*, pending.
(60) Barrett, E. P.; Joyner, L. G.; Halenda, P. P. *J. Am. Chem. Soc.* **1951**, *73*, 373.
(61) Metropolis, N.; Rosenbluth, A. W.; Rosenbluth, M. N.; Teller, A. H.; Teller, E. *J. Chem. Phys.* **1953**, *21*, 1087.
(62) Hriljac, J. A.; Eddy, M. M.; Cheetham, A. K.; Donohue, J. A.; Ray, G. J. *J. Solid State Chem.* **1993**, *106*, 66.
(63) Jorgensen, W. L.; Chandrasekhar, J.; Madura, J. D.; Impey, R. W.; Klein, M. L. *J. Chem. Phys.* **1983**, *79*, 926.
(64) Mayo, S. L.; Olafson, B. D.; Goddard, W. A., III *J. Phys. Chem.* **1990**, *94*, 8897.
(65) Rappe, A. K.; Goddard, W. A., III *J. Phys. Chem.* **1991**, *95*, 3358.
(66) Karasawa, N.; Goddard, W. A., III *J. Phys. Chem.* **1989**, *93*, 7320.
(67) Breck, D. W. *Zeolite Molecular Sieves*; John Wiley & Sons: New York, **1974**.
(68) Müller, U.; Unger, K. K. *Stud. Surf. Sci. Catal.* **1988**, *39*, 101.
(69) Smit, B.; Maesen, L. M. *Nature* **1995**, *374*, 42.
(70) Tchernev, D. *A Waste Heat Driven Automotive Air conditioning System, Int.* Sorption Heat Pump Conference, Munich Germany, **1999**.
(71) Nayak, V. S.; Moffat, J. B.; *J. Phys. Chem.* **1988**, *92*, 7097.
(72) Gupta, A.; Clark, L. A.; Snurr, R. Q. *Langmuir* **2000**, *16*, 3910.
(73) Takaba, H.; Koyama, A.; Nakao, S. *J. Phys. Chem. B* **2000**, *104*, 6353.
(74) Kevan, L.; Narayana, M. *ACS Symp. Ser.* **1983**, *218*, 17.
(75) Kirschhock, C. E. A.; Hunger, B.; Martens, J.; Jacobs, P. A. *J. Phys. Chem. B* **2000**, *104*, 439.
(76) *CRC Handbook of Chemistry and Physics*, 77th ed.; R. Linde, Ed.; CRC Press: 1996−1997.
(77) Izmailova, S. G.; Karetina, I. V.; Khvoshchev, S. S.; Shubaeva, M. A. *J. Colloid Interface Sci.* **1994**, *165*, 318.
(78) Coolidge, A. S. *J. Am. Chem. Soc.* **1924**, *46*, 596.
(79) Coolidge, A. S. *J. Am. Chem. Soc.* **1927**, *49*, 708.
(80) Machin, W. D.; Ross, S. *Proc. R. Soc. London* **1962**, *265*, 455.
(81) Lovas, F. J.; Belov, S. P.; Tretyakov, M. Yu.; Stahl, W.; Suenram, R. D. *J. Mol. Spectrosc.* **1995**, *170*, 478.
(82) Gu, Y.; Kar, T.; Schneider, S. *J. Am. Chem. Soc.* **1999**, *121*, 9411.
(83) Derouane, E. G. *Chem. Phys. Lett.* **1987**, *142*, 200.
(84) Derycke, I.; Vigneron, J. P.; Lambin, Ph.; Lucas, A. A.; Derouane, E. G. *J. Chem.* Phys. **1991**, *94*, 4620.
(85) Ruthven, D. M. *Principles of Adsorption and Adsorption Processes*; John Wiley & Sons: New York, 1984.